

A collection of definitions and fundamentals for a design-oriented inductor model

1st Andrés Vazquez Sieber

* *Departamento de Electrónica*

*Facultad de Ciencias Exactas, Ingeniería y Agrimensura
Universidad Nacional de Rosario (UNR)*

** *Grupo Simulación y Control de Sistemas Físicos
CIFASIS-CONICET-UNR*

Rosario, Argentina
avazquez@fceia.unr.edu.ar

2nd Mónica Romero

* *Departamento de Electrónica*

*Facultad de Ciencias Exactas, Ingeniería y Agrimensura
Universidad Nacional de Rosario (UNR)*

** *Grupo Simulación y Control de Sistemas Físicos
CIFASIS-CONICET-UNR*

Rosario, Argentina
mromero@fceia.unr.edu.ar

Abstract—This paper defines and develops useful concepts related to the several kinds of inductances employed in any comprehensive design-oriented ferrite-based inductor model, which is required to properly design and control high-frequency operated electronic power converters. It is also shown how to extract the necessary parameters from a ferrite material datasheet in order to get inductor models useful for a wide range of core temperatures and magnetic induction levels.

Index Terms—magnetic circuit, ferrite core, major magnetic loop, minor magnetic loop, reversible inductance, amplitude inductance

I. INTRODUCTION

Ferrite-core based low-frequency-current biased inductors are commonly found, for example, in the LC output filter of voltage source inverters (VSI) or step-down DC/DC converters. Those inductors have to effectively filter a relatively low-amplitude high-frequency current being superimposed on a relatively large-amplitude low-frequency current. It is of paramount importance to design these inductors in a way that a minimum inductance value is always ensured which allows the accurate control and the safe operation of the electronic power converter. In order to efficiently design that specific type of inductor, a method to find the required minimum number of turns N_{min} and the optimum air gap length g_{opt} to obtain a specified inductance at a certain current level is needed. This method has to be based upon an accurate inductor model, for which certain inductances and properties need to be defined and explained. Also, these inductance definitions need to be parametrized, among other things, according to the specific ferrite material employed in the core.

The problem of designing such kind of inductors has been widely treated in literature [1], [2], [3], [4]. At the same time, there are many well established definitions of core permeability and inductance [4], [5], [11] according to the actual inductor operating condition. However, it seems that this variety of inductance definitions can be better exploited in order to enhance the inductor design process. In this paper, some specific inductance definitions are revisited and presented under a suitable context for the power electronic

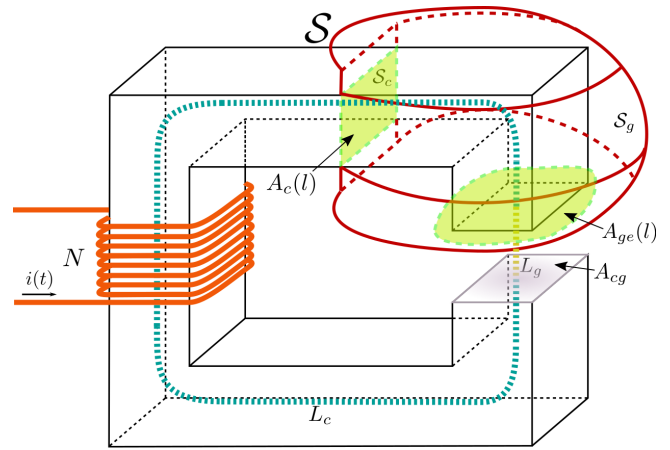


Fig. 1. General magnetic circuit

practitioner. A design-oriented inductor model can be based on the core magnetic model described in this paper which allows to employ the concepts of reversible inductance L_{rev} , amplitude inductance L_a and initial inductance L_i , to further develop an optimized inductor design method. Those inductance definitions rely on their respective core permeabilities, which in this paper are also revisited, contextualized and obtained for two specific ferrite materials: TDK-EPCOS N27 and TDK-EPCOS N87.

This paper is organized as follows. In section II, a general magnetic core model is described and its associated permeabilities are introduced. In section III, definitions of several types of inductances are presented. Section IV shows how to obtain the previously defined permeabilities from the ferrite material datasheet. Section V presents some useful properties of the reversible inductance that could be needed to justify the selection criterion of the inductance value as well as N_{min} and g_{opt} . Finally, conclusions are presented in section VI.

II. MAGNETIC CIRCUIT MODEL

In this section, we obtain a model for the general magnetic circuit considered in Figure 1 using an approach depending on

integration along the mean magnetic path into the ferrite core, L_c and into the air gap, L_g [5]. Suppose that current $i(t)$ can be easily decomposed into a) a component denoted as $i_{LF}(t)$ at a relatively low frequency f_{LF} and b) a component denoted as $i_{HF}(t)$ at a relatively high frequency f_{HF} , with $f_{LF} \ll f_{HF}$. At a certain time \hat{t}_{LF} , i_{LF} reaches its peak value \hat{i}_{LF} and then we have

$$i(t) \approx \hat{i}_{LF} + i_{HF}(t) \quad t \in \left[\hat{t}_{LF} - \frac{1}{f_{HF}}, \hat{t}_{LF} + \frac{1}{f_{HF}} \right] \quad (1)$$

In such a situation, Ampere's law relates the frequency components of current $i(t)$ with their corresponding magnetic field strength H components as follows

$$\begin{aligned} \oint \vec{H}(t, l) d\vec{l} &= \int_{L_c \cup L_g} [\hat{H}_{LF}(l) + H_{HF}(t, l)] dl \\ &= N [\hat{i}_{LF} + i_{HF}(t)] \end{aligned}$$

where $d\vec{l}$ is the path vector, parallel to \vec{H} . Separating the frequency components yields

$$\int_{L_c} \hat{H}_{LF}(l) dl + \int_{L_g} \hat{H}_{LF}(l) dl = N \hat{i}_{LF} \quad (2)$$

$$\begin{aligned} \int_{L_c} H_{HF}(t, l) dl + \int_{L_g} H_{HF}(t, l) dl &= N i_{HF}(t) \\ \int_{L_c} \Delta H_{HF}(l) dl + \int_{L_g} \Delta H_{HF}(l) dl &= N \Delta i_{HF} \end{aligned} \quad (3)$$

where ΔH_{HF} is the amplitude of the field strength excursion due to Δi_{HF} , the amplitude of the high-frequency current excursion during $\frac{1}{f_{HF}}$.

The magnetic induction $B(t, l) = \hat{B}_{LF}(l) + B_{HF}(t, l)$ and its peak-to-peak variation ΔB_{HF} determine the peak induction $\hat{B}(l) = \hat{B}_{LF}(l) + \frac{\Delta B_{HF}(l)}{2}$. These are related to their corresponding field strength $\hat{H}_{LF}(l)$, $H_{HF}(t, l)$, $\Delta H_{HF}(l)$ and $\hat{H}(l)$ according to the medium permeability. Having the air gap paramagnetic properties, along L_g simply hold

$$\frac{\hat{B}_{LF}(l)}{\hat{H}_{LF}(l)} = \frac{B_{HF}(t, l)}{H_{HF}(t, l)} = \frac{\Delta B_{HF}(l)}{\Delta H_{HF}(l)} = \frac{\hat{B}(l)}{\hat{H}(l)} = \mu_0 \quad (4)$$

where μ_0 is the vacuum permeability. In the magnetic core path L_c , those relationships depend on the shape of the ferrite magnetization curve which is shown in Figure 2. It is also the specific major loop that characterizes the behaviour of the ferrite when its magnetic induction evolution spans the two extreme points $\pm B_s$, being B_s the saturation induction. In any inductor, although this situation can be reached with a current i_{LF} having a sufficiently high \hat{i}_{LF} , the actual \hat{i}_{LF} has to be set well below that value since beyond that induction level the core ferrimagnetic properties become severely affected. Starting from a demagnetized core, as \hat{i}_{LF} is gradually increased from zero towards the maximum value causing saturation, the tipping points $(\hat{B}_{LF}, \hat{H}_{LF}$ and $-\hat{B}_{LF}, -\hat{H}_{LF}$) of the ever increasing LF-major loops describe a LF-commutation curve which is also partly shaped by the current magnitude of ΔB_{HF} , due to the memory properties of the ferrite material.

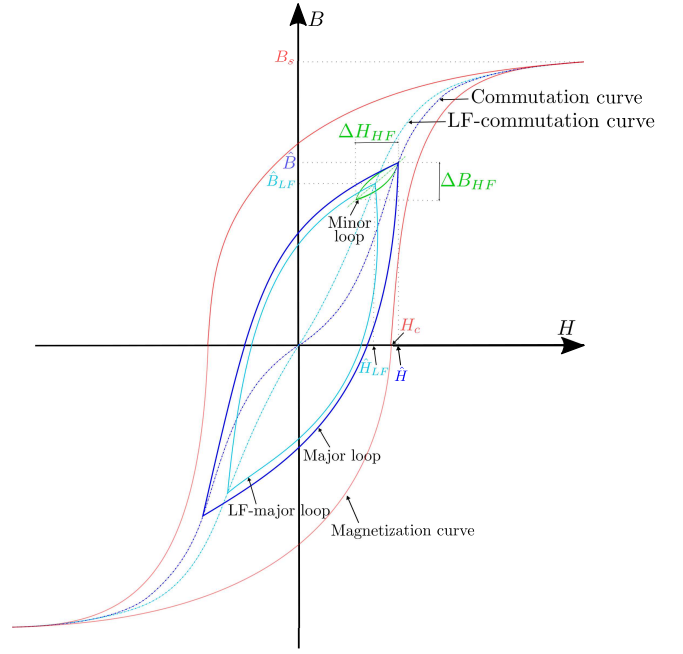


Fig. 2. Ferrite magnetization curve

For any of the points pertaining to that LF-commutation curve, the LF-amplitude permeability μ_a^{LF} is defined as

$$\mu_a^{LF}(\hat{B}_{LF}, \Delta B_{HF}) = \frac{1}{\mu_0} \frac{\hat{B}_{LF}}{\hat{H}_{LF}} \Big|_{\Delta B_{HF}}$$

because it relates only the low frequency amplitude of the magnetic induction and field strength in the ferrite material when the low frequency i_{LF} takes also its amplitude value \hat{i}_{LF} . The magnetic induction generated by i_{LF} will not vary much from \hat{B}_{LF} while t is into the time span defined in (1). Hence during $\frac{1}{f_{HF}}$, $i_{HF}(t)$ will produce an approximately closed minor magnetic loop of amplitude $(\Delta B_{HF}, \Delta H_{HF})$ starting and ending in the neighbourhood of \hat{B}_{LF} , as it is shown in Figure 2. The incremental permeability μ_{Δ} at that quasi-static induction level \hat{B}_{LF} is then defined as

$$\mu_{\Delta}(\hat{B}_{LF}, \Delta B_{HF}) = \frac{1}{\mu_0} \frac{\Delta B_{HF}}{\Delta H_{HF}} \Big|_{\hat{B}_{LF}}$$

Consequently, on L_c holds

$$\hat{H}_{LF}(l) = \frac{\hat{B}_{LF}(l)}{\mu_0 \mu_a^{LF}(\hat{B}_{LF}, \Delta B_{HF})} \quad (5)$$

$$\Delta H_{HF}(l) = \frac{\Delta B_{HF}(l)}{\mu_0 \mu_{\Delta}(\hat{B}_{LF}, \Delta B_{HF})} \quad (6)$$

If ΔB_{HF} is made sufficiently small, then μ_{Δ} and the LF-commutation curve start to be practically independent of ΔB_{HF} . At this point, on the one hand the existing linear

relationship between B_{HF} and H_{HF} is captured by the so-called reversible permeability at \hat{B}_{LF} , $\mu_{r\hat{e}v}$

$$\mu_{r\hat{e}v}(\hat{B}_{LF}) = \lim_{\Delta B_{HF} \rightarrow 0} \mu_{\hat{\Delta}}(\hat{B}_{LF}, \Delta B_{HF})$$

On the other hand, the LF-commutation curve tends to the regular commutation curve and their respective amplitude permeabilities are related as

$$\begin{aligned} \mu_a(\hat{B}) &= \frac{1}{\mu_0} \frac{\hat{B}}{\hat{H}} = \lim_{\substack{\hat{B}_{LF} \rightarrow \hat{B} \\ \Delta B_{HF} \rightarrow 0}} \mu_a^{LF}(\hat{B}_{LF}, \Delta B_{HF}) \\ &= \mu_a(\hat{B}_{LF}) \end{aligned}$$

Now making $\hat{B}_{LF} \rightarrow 0$ due to $\hat{i}_{LF} \rightarrow 0$, the initial permeability μ_i is defined as

$$\mu_i = \lim_{\hat{B}_{LF} \rightarrow 0} \mu_a(\hat{B}_{LF}) = \mu_{r\hat{e}v}(\hat{B}_{LF} = 0)$$

Note that in the core, the relationship between B and H depends not only on the ferrite magnetic characteristics but also on the way in which B evolves with time.

In the magnetic circuit of Figure 1, a closed surface $\mathcal{S} = \mathcal{S}_c \cup \mathcal{S}_g$ that intersects both L_c and L_g paths will satisfy according to Gauss' law that

$$\iint_{\mathcal{S}_c} \vec{B}(t, l) d\vec{S} = \iint_{\mathcal{S}_g} \vec{B}(t, l) d\vec{S} \quad (7)$$

where \mathcal{S}_c is a core cross-section perpendicular to L_c , \mathcal{S}_g is the remaining surface of \mathcal{S} crossing the air gap and $d\vec{S}$ is the area vector of \mathcal{S} . The left side of (7) is the core magnetic flux Φ_c since the magnetic induction there is mainly concentrated into \mathcal{S}_c because $\mu_a, \mu_{\hat{\Delta}} \gg 1$. All the magnetic induction in the air gap will then pass through \mathcal{S}_g , thus the right side of (7) is the air gap magnetic flux Φ_g . Consequently, $\Phi_c = \Phi_g = \hat{\Phi}_{LF} + \Phi_{HF}(t)$. L_c passes perpendicular through the center of \mathcal{S}_c , so the magnetic induction along L_c will be approximately an average of that existing inside \mathcal{S}_c and equal to

$$\hat{B}_{LF}(l) + B_{HF}(t, l) = \frac{\hat{\Phi}_{LF} + \Phi_{HF}(t)}{A_c(l)} \quad (8)$$

where $A_c(l)$ is the area of \mathcal{S}_c at a certain point $l \in L_c$. Around the air gap, the magnetic induction is far more nonuniform in \mathcal{S}_g than in \mathcal{S}_c due to the fringing flux. Thus, the mean induction on L_g can be quite different from the actual values at the edges of the gap, but being a paramagnetic region, it suffices to propose an effective gap area $A_{ge}(l)$ with $l \in L_g$, as if all the induction were there concentrated.

$$\hat{B}_{LF}(l) + B_{HF}(t, l) = \frac{\hat{\Phi}_{LF} + \Phi_{HF}(t)}{A_{ge}(l)} \quad (9)$$

Note that $A_{ge}(l)$ is approximately equal to A_{cg} , the core cross-section in contact with the air gap, if its length is much smaller than the linear dimensions characterizing A_{cg} . Given that the winding turns N embrace practically all Φ_c , it follows that the linkage flux Ψ is

$$\hat{\Phi}_{LF} + \Phi_{HF}(t) = \frac{\hat{\Psi}_{LF} + \Psi_{HF}(t)}{N} \quad (10)$$

The peak linkage flux $\hat{\Psi}$ and magnetic induction $\hat{B}(l)$ in the ferrite core are

$$\hat{\Psi} = \hat{\Psi}_{LF} + \frac{\Delta\Psi_{HF}}{2} \quad (11)$$

$$\hat{B}(l) = \frac{\hat{\Psi}}{NA_c(l)}$$

III. INDUCTANCE DEFINITIONS

Combining (2), (3), (4), (5), (8), (9) and (10) yield the LF-amplitude inductance, L_a^{LF} and the incremental inductance, $L_{\hat{\Delta}}$

$$\begin{aligned} L_a^{LF}(\hat{\Psi}_{LF}, \Delta\Psi_{HF}) &= \frac{\hat{\Psi}_{LF}}{\hat{i}_{LF}} \Big|_{\Delta\Psi_{HF}} \\ &= \frac{N^2}{\mathcal{R}_{c_a}^{LF}(\hat{\Psi}_{LF}, \Delta\Psi_{HF}) + \mathcal{R}_g} \end{aligned} \quad (12)$$

$$\begin{aligned} L_{\hat{\Delta}}(\hat{\Psi}_{LF}, \Delta\Psi_{HF}) &= \frac{\Delta\Psi_{HF}}{\Delta i_{HF}} \Big|_{\hat{\Psi}_{LF}} \\ &= \frac{N^2}{\mathcal{R}_{c_{\hat{\Delta}}}(\hat{\Psi}_{LF}, \Delta\Psi_{HF}) + \mathcal{R}_g} \end{aligned} \quad (13)$$

with

$$\mathcal{R}_{c_a}^{LF}(\hat{\Psi}_{LF}, \Delta\Psi_{HF}) = \int_{L_c} \frac{dl}{\mu_0 \mu_a^{LF} \left(\frac{\hat{\Psi}_{LF}}{NA_c}, \frac{\Delta\Psi_{HF}}{NA_c} \right) A_c(l)} \quad (14)$$

$$\mathcal{R}_{c_{\hat{\Delta}}}(\hat{\Psi}_{LF}, \Delta\Psi_{HF}) = \int_{L_c} \frac{dl}{\mu_0 \mu_{\hat{\Delta}} \left(\frac{\hat{\Psi}_{LF}}{NA_c}, \frac{\Delta\Psi_{HF}}{NA_c} \right) A_c(l)} \quad (15)$$

$$\mathcal{R}_g = \int_{L_g} \frac{dl}{\mu_0 A_{ge}(l)} \quad (16)$$

$\mathcal{R}_{c_a}^{LF}$, $\mathcal{R}_{c_{\hat{\Delta}}}$ and \mathcal{R}_g are the core LF-amplitude reluctance, core incremental reluctance and the air gap reluctance respectively.

Considering the situation where $\Delta\Psi_{HF} \rightarrow 0$, μ_a and $\mu_{r\hat{e}v}$ define the amplitude and reversible inductances at $\hat{\Psi}_{LF}$, L_a and $L_{r\hat{e}v}$, as

$$\begin{aligned} L_a(\hat{\Psi}_{LF}) &= \lim_{\substack{\hat{\Psi}_{LF} \rightarrow \hat{\Psi} \\ \Delta\Psi_{HF} \rightarrow 0}} L_a^{LF}(\hat{\Psi}_{LF}, \Delta\Psi_{HF}) \\ &= \frac{N^2}{\mathcal{R}_{c_a}(\hat{\Psi}_{LF}) + \mathcal{R}_g} \end{aligned} \quad (17)$$

$$\begin{aligned} L_{r\hat{e}v}(\hat{\Psi}_{LF}) &= \lim_{\Delta\Psi_{HF} \rightarrow 0} L_{\hat{\Delta}}(\hat{\Psi}_{LF}, \Delta\Psi_{HF}) \\ &= \frac{N^2}{\mathcal{R}_{c_{r\hat{e}v}}(\hat{\Psi}_{LF}) + \mathcal{R}_g} \end{aligned}$$

$$\mathcal{R}_{c_a}(\hat{\Psi}_{LF}) = \int_{L_c} \frac{dl}{\mu_0 \mu_a \left(\frac{\hat{\Psi}_{LF}}{NA_c} \right) A_c(l)} \quad (18)$$

$$\mathcal{R}_{c_{r\hat{e}v}}(\hat{\Psi}_{LF}) = \int_{L_c} \frac{dl}{\mu_0 \mu_{r\hat{e}v} \left(\frac{\hat{\Psi}_{LF}}{NA_c} \right) A_c(l)} \quad (19)$$

\mathcal{R}_{c_a} and $\mathcal{R}_{c_{r\hat{e}v}}$ are the core amplitude reluctance and the core reversible reluctance respectively.

L_a and $L_{r\hat{e}v}$ usually have dissimilar values at a same $\hat{\Psi}_{LF}$ and vary differently as $\hat{\Psi}_{LF}$ increases from zero to relatively high values. It is then important to find a common situation to relate and relativize their current values with. In a demagnetized material, μ_a and $\mu_{r\hat{e}v}$ coincide at the origin which means that L_a and $L_{r\hat{e}v}$ converge to the initial inductance L_i

$$L_i = \lim_{\hat{\Psi}_{LF} \rightarrow 0} L_a(\hat{\Psi}_{LF}) = L_{r\hat{e}v}(\hat{\Psi}_{LF} = 0) = \frac{N^2}{\mathcal{R}_{c_i} + \mathcal{R}_g} \quad (20)$$

$$\mathcal{R}_{c_i} = \int_{L_c} \frac{dl}{\mu_0 \mu_i A_c(l)} \quad (21)$$

being \mathcal{R}_{c_i} the core initial reluctance. Note that only μ_i does not vary with the core cross-sectional area $A_c(l)$ along the magnetic path. However, μ_i as well as μ_a and $\mu_{r\hat{e}v}$ do depend heavily on the core temperature, as is modeled in the next section.

IV. PERMEABILITY MODELS

The dependence of \mathcal{R}_{c_a} in (18) and \mathcal{R}_{c_i} in (21) from core temperature T_c and magnetic induction $\hat{B}_{LF} = \hat{B}$, in each specific part of the core, is addressed when the corresponding functions $\mu_a(\hat{B}_{LF}, T_c)$ and $\mu_i(T_c)$ are extracted from the ferrite material datasheet [12] [13]. Permeability μ_a is a function of magnetic induction amplitude \hat{B} and core temperature (3-D lookup table) and permeability μ_i is a function of core temperature (2-D lookup table). To get the best accuracy in the inductor model, the μ_a curve given by the ferrite manufacturer should have been obtained at a frequency close to f_{LF} .

The temperature and induction dependence of $\mathcal{R}_{c_{r\hat{e}v}}$ in (19) is subjected to find $\mu_{r\hat{e}v}(\hat{B}_{LF}, T_c)$. In [6] it is concluded that the commutation curve coincides with the so-called initial magnetization curve for soft ferrite materials, that is $(B_{DC}, H_{DC}) = (\hat{B}, \hat{H})$. This means that $\mu_{r\hat{e}v}$ is equal to DC-biased μ_{rev} which can be extracted from a graph or as a function of DC-bias field strength H_{DC} . That curve may not be given in datasheets for a particular ferrite material or for the core temperatures at which $\mu_{r\hat{e}v}$ has to be obtained, but even if it were available it should be put in terms of \hat{B}_{LF} to be employed in (19). To overcome these limitations, we use a permeability model directly relating DC-biased μ_{rev} with DC-bias magnetic induction B_{DC} [7], where all its parameters at the desired core temperature can be entirely obtained from any ferrite datasheet, in the way it is next explained. This approach has been experimentally validated for many ferrite materials operating at different temperatures [8] and it is currently employed by major ferrite manufacturers [9].

Let us first consider the empirical models that curvefit the upper (u) and lower (l) branches of the dynamic magnetization

(B-H) curve of Figure 2 [7],

$$H_u(B) = \frac{B}{\mu_0 \mu_c} \frac{1}{1 - \left(\frac{B}{B_s}\right)^{a_u}} - H_c \quad (22)$$

$$H_l(B) = \frac{B}{\mu_0 \mu_c} \frac{1}{1 - \left(\frac{B}{B_s}\right)^{a_l}} + H_c \quad (23)$$

with the positive parameters: coercive field strength H_c , coercive permeability μ_c and squareness coefficients a_u and a_l for each branch. Supposing that $a_l \approx a_u$ and being $\hat{B} = \hat{B}_{LF}$, $\mu_{r\hat{e}v}(\hat{B}_{LF}, T_c)$ can be expressed as [7]

$$\mu_{r\hat{e}v}(\hat{B}_{LF}, T_c) = \left\{ \frac{1 + (a_l - 1) \left(\frac{\hat{B}_{LF}}{B_s}\right)^{a_l}}{\left[1 - \left(\frac{\hat{B}_{LF}}{B_s}\right)^{a_l}\right]^2} \frac{1}{\mu_c} + \frac{b_o}{\left(1 - \frac{\hat{B}_{LF}}{B_s}\right) \left[2 - \left(1 - \frac{\hat{B}_{LF}}{B_s}\right)^{a_o}\right]} \right\}^{-1} \quad (24)$$

$$a_o = \frac{b_o B_s}{\mu_0 H_c} \quad b_o = \frac{1}{\mu_i} - \frac{1}{\mu_c}$$

Apart from μ_i , $\mu_{r\hat{e}v}$ depends on T_c through B_s , H_c , a_l and μ_c and thus (23) has to be numerically fitted for each particular T_c . The fitting data is obtained from the 3-D lookup table $H(B, T = T_c)$ based on the corresponding curves from the ferrite material datasheet [12] [13].

The starting guess points for the fitting process are extracted from 2-D lookup tables $B_s^*(T)$, $H_c^*(T)$, $a_l^*(T)$ and $\mu_c^*(T)$. $B_s^*(T)$ and $H_c^*(T)$ are built to linearly interpolate the two saturation induction and coercive field strength values (B_{s1} , B_{s2} , H_{c1} and H_{c2} respectively), that are stated at the two corresponding temperatures T_1 , T_2 , in the datasheet of the magnetic material. Lookup tables $a_l^*(T)$ and $\mu_c^*(T)$ are conformed in the following way. Let $H_{11}(B_{11}, T_1)$ and $H_{12}(B_{12}, T_1)$ be the field strength at two different induction levels from the lower branch of the B-H curve at temperature T_1 given by the datasheet. The value B_{11} could be from the "linear" region of the curve, while B_{12} could be taken from the "knee" between "linear" and "saturation" regions of the curve at temperature T_1 . The estimations of coefficients a_l and μ_c from (23) at temperature T_1 , a_{l1}^* and μ_{c1}^* respectively, are found numerically solving

$$\frac{1 - \left(\frac{B_{11}}{B_{s1}}\right)^{a_{l1}^*}}{1 - \left(\frac{B_{12}}{B_{s1}}\right)^{a_{l1}^*}} = \frac{H_{12} - H_{c1} B_{11}}{H_{11} - H_{c1} B_{12}}$$

$$\mu_{c1}^* = \frac{1}{\mu_0} \frac{B_{11}}{H_{11} - H_{c1}} \frac{1}{1 - \left(\frac{B_{11}}{B_{s1}}\right)^{a_{l1}^*}}$$

Using the B-H curve at temperature T_2 , a_{l2}^* and μ_{c2}^* can be also obtained following a similar reasoning. Finally, $a_l^*(T)$ and $\mu_c^*(T)$ are built to linearly interpolate a_{l1}^* , a_{l2}^* and μ_{c1}^* , μ_{c2}^*

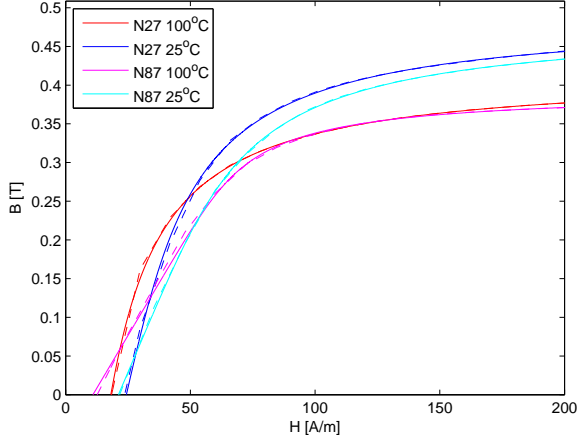


Fig. 3. Curve-fitting of the lower branch of the magnetization loops (first quadrant) for materials N27 and N87. Dashed lines are interpolated data from datasheet

respectively. Figure 3 shows the fitting goodness of (23) for TDK-EPCOS ferrite materials N27 and N87 while their corresponding parameters for using (24) are summarized in Table I. To get the best accuracy in the inductor model, the magnetization curve given by the ferrite manufacturer should have been obtained at a frequency close to f_{HF} .

TABLE I
REVERSIBLE PERMEABILITY $\mu_{r\hat{e}v}$ MODEL PARAMETERS (EQUATION (24))

Material	T_c [$^{\circ}C$]	a_l	H_c [A/m]	μ_c	μ_i	B_s [T]
N27	100	1.25	18.12	14079	3231	0.4165
N27	25	2.00	24.35	11154	1700	0.4895
N87	100	8.00	10.94	4330	3976	0.3925
N87	25	3.78	21.17	6014	2210	0.4803

V. CONSIDERATIONS ON THE REVERSIBLE INDUCTANCE

Recall that if $\Delta\Psi_{HF} \rightarrow 0$ we can consider

$$L_{r\hat{e}v}(\hat{\Psi}) = L_{\hat{\Delta}}(\hat{\Psi}_{LF}, \Delta\Psi_{HF}) = L_{r\hat{e}v}(\hat{\Psi}_{LF})$$

It is important to remark that in this situation $L_{r\hat{e}v}$ is the minimum value of reversible inductance arising along the whole symmetric major loop having $\pm(\hat{H}_{LF}, \hat{B}_{LF})$ as tipping points. This is in fact proved by taking into consideration the upper branch of the particular $\pm(\hat{H}_{LF}, \hat{B}_{LF})$ major loop which can be described in terms of (22)-(23) as [6]

$$H_u^{LF}(B) = H_u(B) + \frac{[\hat{H}_{LF} - H_u(\hat{B}_{LF})]^\beta}{[\hat{H}_l(\hat{B}_{LF}) - \hat{H}_{LF}]^\alpha} \quad (25)$$

$$\alpha = \frac{B - \hat{B}_{LF}}{2\hat{B}_{LF}} \quad \beta = \frac{B + \hat{B}_{LF}}{2\hat{B}_{LF}}$$

and its first derivative, the inverse of the so-called differential permeability μ_d [4]

$$\frac{dH_u^{LF}}{dB} = \frac{1}{\mu_d}$$

Since $\mu_{rev} < \mu_d$ [4] it is sufficient to show that $\frac{d\mu_d}{dB} < 0$ to conclude that L_{rev} is decreasing when B takes values from zero to \hat{B}_{LF} and hence $L_{r\hat{e}v}$ is the absolute minimum. Accordingly,

$$\frac{d\mu_d}{dB} = -\mu_d^2 \frac{d^2 H_u^{LF}}{dB^2}$$

$$\frac{d^2 H_u^{LF}}{dB^2} = \frac{a_u \left(\frac{B}{B_s}\right)^{a_u} \left[1 - \left(\frac{B}{B_s}\right)^{a_u} + a_u + a_u \left(\frac{B}{B_s}\right)^{a_u}\right]}{\mu_0 \mu_c \left[1 - \left(\frac{B}{B_s}\right)^{a_u}\right]^3 B}$$

$$+ \left[\frac{\ln \frac{H_l(\hat{B}_{LF}) - \hat{H}_{LF}}{\hat{H}_{LF} - H_u(\hat{B}_{LF})}}{2\hat{B}_{LF}} \right]^2 \frac{[\hat{H}_{LF} - H_u(\hat{B}_{LF})]^\beta}{[\hat{H}_l(\hat{B}_{LF}) - \hat{H}_{LF}]^\alpha} \quad (26)$$

\hat{H}_{LF} is inside the area delimited by the largest major loop, the magnetization curve, that is described by (22)-(23). Consequently, (26) is positive for $B \in [0, \hat{B}_{LF}]$ and thus μ_d is ever decreasing for increasing values of $B > 0$.

Now suppose that gradually $\Delta\Psi_{HF}$ is increased and $\hat{\Psi}_{LF}$ is decreased in such a way that $\hat{\Psi}$ remains unchanged, implying that \hat{B} and \hat{H} are unmodified in all parts of the core. This scenario brings into existence increasingly asymmetric minor loops in the $B - H$ plane with tipping points

$$\hat{B} = \hat{B}_{LF} + \frac{\Delta B_{HF}}{2}$$

$$\hat{H} = \hat{H}_{LF} + k_H \Delta H_{HF}$$

$$\hat{B} - \Delta B_{HF} = \hat{B}_{LF} - \frac{\Delta B_{HF}}{2}$$

$$\hat{H} - \Delta H_{HF} = \hat{H}_{LF} - (1 - k_H) \Delta H_{HF}$$

being $k_H \in [0.5, 1)$ the magnetic field symmetry factor. Considering that along a general magnetic loop μ_d increases as B decreases, it can be stated that

$$\hat{B} - \frac{dB}{dH} \Big|_{\hat{B}} \Delta H_{HF} \geq \hat{B} - \Delta B_{HF}$$

and hence

$$\mu_{r\hat{e}v}(\hat{B}) \leq \mu_d(\hat{B}) \leq \mu_{\hat{\Delta}}(\hat{B}_{LF}, \Delta B_{HF})$$

Inside the minor loop, we can define the minor-loop amplitude permeability μ_a^{MN} as

$$\mu_a^{MN} = \frac{1}{\mu_0} \frac{\hat{B} - \hat{B}_{LF}}{\hat{H} - \hat{H}_{LF}} = \frac{1}{\mu_0} \frac{\Delta B_{HF}}{2k_H \Delta H_{HF}} = \frac{1}{2k_H} \mu_{\hat{\Delta}}$$

and to note that it holds $\mu_{r\hat{e}v}(\hat{B}) < \mu_{r\hat{e}v}(\hat{B}_{LF})$, since when B is far from the origin, $\mu_{r\hat{e}v}$ decreases as B increases. Consequently,

$$\hat{B}_{LF} + \mu_0 \mu_{r\hat{e}v}(\hat{B}_{LF}) k_H \Delta H_{HF} \geq \hat{B}_{LF} + \frac{\Delta B_{HF}}{2}$$

and hence

$$\mu_{r\hat{e}v}(\hat{B}_{LF}) \geq \mu_a^{MN} \leq \mu_{\hat{\Delta}}$$

If the minor loop keeps some degree of symmetry around $(\hat{B}_{LF}, \hat{H}_{LF})$, i.e. $k_H \approx 0.5$, then $\mu_a^{MN} \approx \mu_{\hat{\Delta}}$ and hence

$$\mu_{r\hat{e}v}(\hat{B}) \leq \mu_{\hat{\Delta}}(\hat{B}_{LF}, \Delta B_{HF}) \leq \mu_{r\hat{e}v}(\hat{B}_{LF})$$

However, that minor loop with tipping points

$$(\hat{B}, \hat{H}); (\hat{B} - \Delta B_{HF}, \hat{H} - \Delta H_{HF})$$

and an enclosing symmetric major loop with tipping points

$$(\hat{B}, \hat{H}); (-\hat{B}, -\hat{H})$$

coincide in the vicinity of their uppermost tipping point (\hat{B}, \hat{H}) [10] [7]. Hence, $\mu_{r\hat{e}v}(\hat{B})$ at the existing minor loop is equal to $\mu_{r\hat{e}v}(\hat{B})$ at that hypothetical major loop. In fact, $\mu_{rev}(B_{DC})$ [7], from which (24) is particularly derived, depends on the current magnetic induction value regardless its previous evolution [11]. Note that from the minor loop standpoint, $\hat{\Psi}$ is given by (11), but it can be also put in terms of the amplitude permeability as

$$\begin{aligned} \hat{\Psi} &= L_a(\hat{\Psi})\hat{i} \\ \hat{i} &= \max_t(\hat{i}_{LF} + i_{HF}(t)) \end{aligned}$$

and thus it is valid

$$\begin{aligned} L_a\left(\hat{\Psi}_{LF} + \frac{\Delta\Psi_{HF}}{2}\right)\hat{i} &= L_a^{LF}\hat{i}_{LF} + \frac{\Delta\Psi_{HF}}{2} \\ L_a^{LF} &= L_a^{LF}(\hat{\Psi}_{LF}, \Delta\Psi_{HF}) \end{aligned}$$

On that enclosing symmetric major loop, characterized by parameters $\hat{\Psi}^{MJ}$, \hat{i}_{LF}^{MJ} and \hat{i}^{MJ} , we have that

$$\begin{aligned} \hat{\Psi}^{MJ} &= L_a(\hat{\Psi}^{MJ})\hat{i}^{MJ} = \hat{\Psi} \\ \hat{i}^{MJ} &= \hat{i}_{LF}^{MJ} = \hat{i} \end{aligned}$$

Consequently, for $\Delta\Psi_{HF} > 0$ we get

$$\begin{aligned} L_{r\hat{e}v}(\hat{\Psi}^{MJ}) &= L_{r\hat{e}v}(\hat{\Psi}) < L_{\hat{\Delta}} < L_{r\hat{e}v}(\hat{\Psi}_{LF}) \quad (27) \\ L_{\hat{\Delta}} &= L_{\hat{\Delta}}(\hat{\Psi}_{LF}, \Delta\Psi_{HF}) \end{aligned}$$

VI. CONCLUSION

The objective of this paper is to provide a collection of basic definitions and properties to ground a comprehensive ferrite-core based low-frequency-current biased inductor model for an optimized design method, which is a fundamental tool to properly design and control any type of electronic power converter. The same procedures followed to extract the required parameters of N27 and N87 materials can be easily adapted to obtain that data for other ferrite materials.

ACKNOWLEDGMENT

The first author wants to thank Dr. Hernan Haimovich for his guidance and constructive suggestions.

REFERENCES

- [1] C. Wm. T. McLyman, *Transformer and Inductor Design Handbook*, 3rd ed. New York, USA: Marcel-Dekker, 2004.
- [2] N. Mohan, T. M. Undeland and W. P. Robbins, *Power Electronics. Converters, Applications, and Design*, 3rd ed. New York, USA: John Wiley & Sons, 2003.
- [3] M. K. Kazimierczuk, *High-Frequency Magnetic Components*, 2nd ed. West Sussex, England: John Wiley & Sons, 2014.
- [4] A. Van den Bossche and V. C. Valchev, *Inductors and Transformers for Power Electronics*, 1st ed. Boca Raton, USA: Taylor & Francis, 2005.
- [5] E. C. Snelling, *Soft Ferrites. Properties and Applications*, 1st ed. London, England: Iliffe Books Ltd, 1969.
- [6] M. Esguerra, *Computation of minor hysteresis loops from measured major loops*, Journal of Magnetism and Magnetic Materials, no. 157/158, pp. 366-368, Elsevier Science B.V., 1996.
- [7] M. Esguerra, *Modelling Hysteresis loops of Soft Ferrite Materials*, in Proc. of the International Conference on Ferrites ICF 8, Kyoto, Japan, pp. 220-220, Sep. 2000.
- [8] M. Esguerra, M. Rottner and S. Goswami, *Calculating Major Hysteresis loops from DC-biased Permeability*, in Proc. of the International Conference on Ferrites ICF 9, San Francisco, USA, Aug. 2004.
- [9] M. Esguerra, *Magnetics Design Tool for Power Applications*, Bodo's Power Systems, pp. 42-46, Apr. 2015. [Online]. Available: www.bodospower.com/restricted/downloads/bp_2015_04.pdf.
- [10] R. G. Harrison, *Modeling High-Order Ferromagnetic Hysteretic Minor Loops and Spirals Using a Generalized Positive-Feedback Theory*, in IEEE Transactions on Magnetics, vol. 48, no. 3, pp. 1115-1129, March 2012.
- [11] C. Heck, *Magnetic Materials and their Applications*, 1st ed. London, England: Butterworth, 1974.
- [12] EPCOS AG, *SIFERRIT material N27*, Ferrite and Accessories, May 2017. [Online]. Available: www.tdk-electronics.tdk.com/download/528850/d7dcd087c9a2dbd3a81365841d4aa9a5/pdf-n27.pdf
- [13] EPCOS AG, *SIFERRIT material N87*, Ferrite and Accessories, Sep 2017. [Online]. Available: www.tdk-electronics.tdk.com/download/528882/71e02c7b9384de1331b3f625ce4b2123/pdf-n87.pdf